

# We are IntechOpen, the world's leading publisher of Open Access books Built by scientists, for scientists

6,900

Open access books available

185,000

International authors and editors

200M

Downloads

Our authors are among the

154

Countries delivered to

TOP 1%

most cited scientists

12.2%

Contributors from top 500 universities



WEB OF SCIENCE™

Selection of our books indexed in the Book Citation Index  
in Web of Science™ Core Collection (BKCI)

Interested in publishing with us?  
Contact [book.department@intechopen.com](mailto:book.department@intechopen.com)

Numbers displayed above are based on latest data collected.  
For more information visit [www.intechopen.com](http://www.intechopen.com)



---

# Looking into Metal-Organic Frameworks with Solid-State NMR Spectroscopy

---

Gregor Mali

Additional information is available at the end of the chapter

<http://dx.doi.org/10.5772/64134>

---

## Abstract

Nuclear magnetic resonance (NMR) spectroscopy is a powerful tool for characterization of materials. It can detect local structure around selected atomic nuclei and provide information on the dynamics of these nuclei. In case of metal-organic frameworks, NMR spectroscopy can help elucidate the framework structure, locate the molecules adsorbed into the pores, and inspect and characterize the interactions of these molecules with the frameworks. The present chapter discusses selected recent examples of solid-state NMR studies that provide valuable insight into the structure and function of metal-organic frameworks.

**Keywords:** MAS NMR, organic linker, metal centre, molecules within pores, short-range order, disorder, mixed-linker MOFs

---

## 1. Introduction

Preparing the most efficient metal-organic framework materials (MOFs) for selected applications requires not only knowledge about the atomic-scale structures of these MOFs but also understanding of the atomic-scale processes during the action of MOFs in catalysis, gas separation and storage, drug delivery, etc. In order to gain this knowledge and this understanding, it is mandatory that MOFs are inspected by a set of complementary techniques that elucidate short- and long-range structural motifs, static and dynamic properties, interactions among the frameworks and the adsorbates. That is why, in addition to the very well established thermal, sorption and diffraction analyses, modeling and spectroscopic investigations are becoming more and more important in the studies of MOFs.

---

Among the spectroscopic techniques, solid-state nuclear magnetic resonance (NMR) is one of the most powerful characterization techniques, because it can provide element-specific atomic-resolution insight into materials. It can be used at many different stages of research connected to MOFs; from studies of their formation, their structure determination, to in-situ studies of their performance. As a local spectroscopic tool, solid-state NMR is complementary to diffraction techniques that rely on the existence of long-range order and that provide a picture of an average crystal structure. NMR experiments can prove or disprove the hypotheses proposed by modeling, predicting preferential adsorption sites and estimating strength of interactions between the adsorbed molecules and the MOF matrices. It can follow gradual adsorption or desorption of molecules into pores, locate and quantify these molecules, and thus complement the data obtained by the thermal and sorption analyses. Solid-state NMR is also extremely important for studying dynamics of the frameworks and of the adsorbed molecules. Therefore, employing NMR spectroscopy is crucial for deducing the structure-to-function relationships of MOFs.

The present chapter begins with a short introduction into solid-state NMR spectroscopy. Here, the basic characteristics of NMR and the most important techniques and recent methodological developments for studying the framework and the adsorbed molecules are briefly mentioned. NMR spectroscopy is particularly important for studying motifs in MOFs that do not exhibit long-range order. Such motifs can be found in the frameworks themselves, especially when one is dealing with mixed-linker or mixed-metal MOFs, and when the molecules within the pores do not occupy equal positions within each unit cell. The second section of the chapter presents some interesting and representative examples of NMR studies of frameworks of the metal-organic materials. For example, in case of mixed-linker MOFs two recent studies demonstrate that solid-state NMR is the only technique, which not only proves or disproves the incorporation of different linkers into the framework, but also provides an answer about the distribution of different linkers within the frameworks. The third, largest section of the chapter is devoted to the application of NMR spectroscopy for studying the molecules adsorbed into the pores of MOFs. These molecules can be solvent molecules, which remain trapped in MOFs after the synthesis and can play a stabilizing role in these materials, or can be molecules adsorbed during the application of MOFs in catalysis, in gas separation and storage, in energy storage, and in drug-delivery.

The chapter does not attempt to present a complete review of the solid-state NMR studies on MOFs, but focuses on prominent recent examples and discusses their impact on the understanding of the properties and functioning of MOFs. Some other, more extensive reviews on NMR spectroscopy of MOFs can be found in literature [1, 2].

## 2. Briefly about solid-state NMR spectroscopy

Atomic nuclei with nonzero magnetic dipole moment and atomic nuclei with nonzero electric quadrupole moment are extremely sensitive probes capable of detecting tiny differences in local magnetic and local electric fields. Local magnetic field at the position of an atomic nucleus

depends on the electric currents in the vicinity of this nucleus and on the number and geometrical arrangement of magnetic moments in its neighborhood. A strong external magnetic field, which is in a modern NMR spectrometer generated by a superconducting magnet, induces electric current in the cloud of electrons that is surrounding an atomic nucleus. This electric current gives rise to a local magnetic field that partially shields the external magnetic field. We are talking about chemical shielding and chemical shift, because the extent of shielding and the consequent shift of the spectral line in the NMR spectrum depend on the chemical environment of the atomic nucleus. With chemical environment we mean the nature and the number of neighbors in the first and second coordination shells, and the nature, strength and angles of the nearest chemical bonds. For example, chemical shielding and the resulting local magnetic fields are not equal at the positions of  $^{13}\text{C}$  nuclei in  $\text{CH}_4$  and in  $\text{CH}_3\text{OH}$ ; consequently, the  $^{13}\text{C}$  NMR signals of  $\text{CH}_4$  and  $\text{CH}_3\text{OH}$  resonate at different frequencies.

As mentioned above, the second important contribution to the local magnetic field at the position of an atomic nucleus is the contribution of the neighboring atomic nuclei with nonzero magnetic moments. Each atomic nucleus with a magnetic moment acts as a tiny source of magnetic field in a similar way as a bar magnet generates magnetic field in its surroundings. What is particularly important with such magnetic fields is that their strengths depend strictly on the distances between the atomic nuclei that generate the fields and the atomic nucleus that detects these fields. We say that a pair of proximal nuclei is coupled through the magnetic dipolar coupling. With the advanced NMR experiments we can exploit this dipolar coupling for obtaining qualitative or sometimes even quantitative information about the interatomic distance.

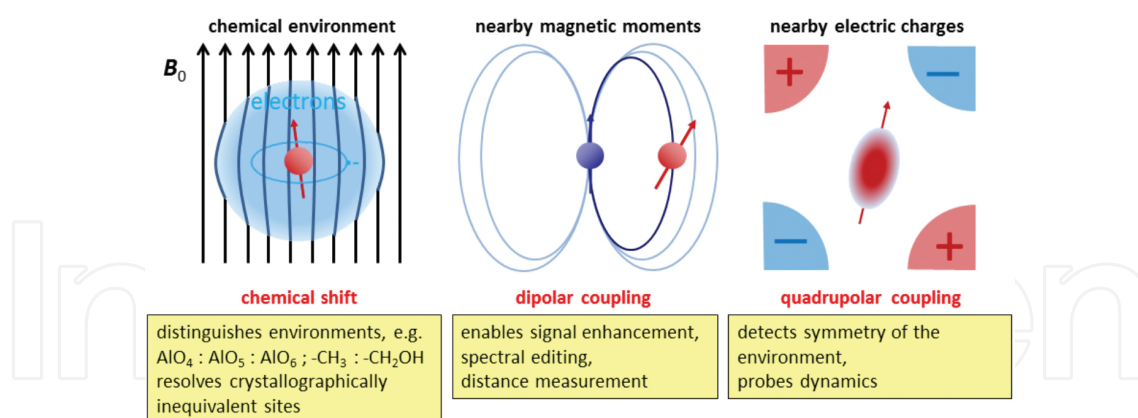


**Figure 1.** Summary of the most important interactions, detected by NMR, and of the available information.

Local electric field at the position of an atomic nucleus depends on the arrangement of electric charges in the neighborhood of the nucleus. In fact, NMR spectroscopy detects electric field gradients to which only the nonspherical atomic nuclei are sensitive. These nuclei are often called quadrupolar nuclei and they all have spin quantum number larger than  $\frac{1}{2}$ . The sensitivity of quadrupolar nuclei to the local electric field gradients can provide useful information on the symmetry of the environments around them. Measurement of the

magnitude of the electric field gradient (the strength of the electric quadrupolar interaction) can also yield an insight into the dynamics of the species in which the atomic nuclei are located, that is, for example, into the dynamics of a framework or a molecule. **Figure 1** schematically shows the most important sources of local fields detectable by solid-state NMR. The figure also briefly summarizes the information that is offered by chemical shifts, dipolar couplings, and electric quadrupolar interactions.

The magnitude and the direction of a local magnetic field do not depend only on the molecular or crystalline environment, but also on the orientation of the molecule or the crystal fragment with respect to the direction of the external magnetic field. For example, chemical shieldings in a phenyl ring that is perpendicular to the external magnetic field and in a phenyl ring that is parallel to the external magnetic field will differ from one another, because the induced electric currents in the rings will be different. When studying materials, we are very often dealing with powders in which the particles are oriented in many different directions. This means that, for example, atomic nuclei at equal crystallographic sites but in differently oriented crystallites will detect different local fields. In an NMR spectrum of such a powder, the corresponding NMR signal will reflect the distribution of the local fields and will appear as a broad distributed line, which is called a powder pattern. In this respect, NMR spectra of powders are very much different from the NMR spectra of solutions. In solutions, due to fast motion and reorientation of molecules, atomic nuclei detect orientationally averaged local fields and NMR spectra exhibit very sharp signals. We say that in solutions, NMR detects only the isotropic contributions to the local fields. The resolution of the obtained NMR spectra is excellent and the detection of tiny differences in chemical environments is easy. As opposed to that, the resolution in solid-state NMR spectra of powdered materials is very poor, because the broad powder patterns overlap extensively. In order to improve resolution and thus to gain more information about the inequivalent sites in materials, we try to mimic fast molecular reorientations by spinning powdered samples very quickly. Indeed, fast spinning about the axis that is inclined from the direction of the external magnetic field by  $54.7^\circ$  improves resolution of NMR spectra of powders drastically. The special angle mentioned above is called the magic angle and the method is named magic angle spinning (MAS) [3]. MAS is the basis of almost all modern solid-state NMR experiments.

Apart from attempts for improving spectral resolution, solid-state NMR faces two other major technical challenges. The first is how to increase the NMR signal, which is very weak compared to signals of other spectroscopies. One of routinely employed approaches to achieve that is the usage of cross polarization (CP) step [4]. With this step, the signal of the selected atomic nuclei is enhanced via the transfer of spin polarization from atomic nuclei with larger magnetic moments. For example,  $^1\text{H}$  nuclei have four- and ten-times as large magnetic moment as  $^{13}\text{C}$  and  $^{15}\text{N}$  nuclei, respectively, thus the application of  $^1\text{H}$ - $^{13}\text{C}$  and  $^1\text{H}$ - $^{15}\text{N}$  CP approach can greatly enhance  $^{13}\text{C}$  and  $^{15}\text{N}$  NMR signals. The method is most efficient if both types of atomic nuclei have spin quantum number of  $\frac{1}{2}$  and if the nuclei are coupled with strong dipolar coupling (i.e., if the nuclei of the two types are proximal one to another). The above listed nuclei  $^1\text{H}$ ,  $^{13}\text{C}$ , and  $^{15}\text{N}$  all have spin equal to  $\frac{1}{2}$ . Because they are the major constituents of the organic linkers



in MOFs and of many molecules that are adsorbed within MOFs (small organic molecules, drug molecules), CP-MAS-based experiments are regularly employed for studying MOFs.

NMR-active nuclei in the inorganic metal-oxo vertices in MOFs are typically quadrupolar nuclei, that is nuclei with spin larger than  $\frac{1}{2}$ . Among them,  $^{27}\text{Al}$ ,  $^{45}\text{Sc}$ , and  $^{51}\text{V}$  are abundant and have moderately large magnetic moments, therefore NMR spectroscopy of these nuclei is very sensitive. In majority of other cases, such as in case of  $^{25}\text{Mg}$ ,  $^{67}\text{Zn}$ , or  $^{91}\text{Zr}$ , we are dealing with low-abundance nuclei and/or with nuclei with small magnetic moments, with which NMR spectroscopy is very demanding. Increasing the NMR signal of these nuclei is often attempted through the acquisition of the Carr-Purcell-Meiboom-Gill (CPMG) train of echoes [5], and through the usage of strong external magnetic fields and large amounts of samples. Additionally, because spectral lines of quadrupolar nuclei can be very wide, broadbanded WURST (Wideband, Uniform Rate, and Smooth Truncation) or similar type of excitation is often needed [6].

Even WURST-CPMG and strong magnetic fields are usually not sufficient for a successful NMR spectroscopy of oxygen nuclei. Because the NMR-active isotope  $^{17}\text{O}$  is a very rare isotope of oxygen, only 0.04% abundant in nature, practical  $^{17}\text{O}$  NMR spectroscopy relies on isotopic enrichment of samples. Isotopic enrichment can be useful or even necessary also when measuring  $^{13}\text{C}$  or  $^{15}\text{N}$  NMR spectra of adsorbed molecules, especially if these molecules are present in small concentrations within MOFs and if CP via  $^1\text{H}$  nuclei is not possible (either because the molecules do not contain hydrogen atoms, or because the dipolar coupling with  $^1\text{H}$  nuclei is motionally averaged out). Typical examples of NMR studies of isotopically enriched molecules are studies of  $^{13}\text{CO}_2$  molecules within the pores of MOFs. **Table 1** lists selected physical properties for atomic nuclei (isotopes) that are most often employed as probes in NMR spectroscopy of MOFs.

Isotope	Ground state spin	Natural abundance	NMR frequency at 14.10 T/MHz
$^1\text{H}$	1/2	~100%	600.00
$^2\text{H}$	1	0.015%	92.10
$^{13}\text{C}$	1/2	1.1%	150.87
$^{15}\text{N}$	1/2	0.37%	60.82
$^{17}\text{O}$	5/2	0.04%	81.34
$^{25}\text{Mg}$	5/2	10%	36.73
$^{27}\text{Al}$	5/2	100%	156.34
$^{67}\text{Zn}$	5/2	3.1%	37.54
$^{91}\text{Zr}$	5/2	11%	55.78

**Table 1.** Selected properties of nuclear isotopes, which are frequently encountered in MOFs.

The third technical challenge of solid-state NMR spectroscopy is how to extract the information about the selected internuclear distances. In case of MOFs, these could be the distances

among the atomic nuclei of the adsorbed molecules and the atomic nuclei within the frameworks. As mentioned above, the information on the distances is contained in the magnitude of the dipolar coupling between these nuclei. However, because dipolar coupling is an anisotropic interaction, it is very efficiently suppressed or entirely averaged out by MAS. To keep the enhanced resolution of NMR spectra obtainable by MAS, but still to be able to detect the magnitude of the dipolar coupling among the selected nuclei, several recoupling techniques were developed and were included into different types of homonuclear and heteronuclear correlation experiments. Homonuclear correlation experiments, like  $^1\text{H}$ - $^1\text{H}$  correlation experiments, most often exploit spin diffusion enhanced by RFDR (Radio-Frequency-driven Dipolar Recoupling) [7], or recoupling of the dipolar interaction by BABA or POST-C7 pulse sequences [8, 9]. Heteronuclear dipolar couplings, like  $^1\text{H}$ - $^{13}\text{C}$  couplings, can be probed qualitatively by various two-dimensional HETCOR (HETero-nuclear CORrelation) experiments [10, 11] or quantitatively by the REDOR-type pulse sequences [12].

In the above discussion of local magnetic fields, we have skipped a contribution that is often quite important in MOFs. It is the contribution of paramagnetic centers, such as Cr, Mn, Fe, Co, Ni, and Cu centers. Unpaired electrons of these centers have much larger magnetic moments than atomic nuclei and therefore drastically affect the NMR spectra of neighboring nuclei. In powders, the strong dipolar interaction with unpaired electrons leads to very fast nuclear spin-lattice relaxation and to huge line broadening of NMR signals. These effects depend on the geometrical arrangement of the unpaired electrons around an atomic nucleus and again offer some information on the distances between the paramagnetic centers and atomic nuclei. If electronic spin polarization is through bonds transferred to the position of an atomic nucleus, the so-called hyperfine electron-nucleus interaction has to be taken into account. This interaction can be very strong and can severely shift NMR lines. For example, for nuclei that are two bonds apart from the paramagnetic metal centre (e.g., for  $^{13}\text{C}$  in the  $-\text{C}-\text{O}-\text{Cu}$  motif), the shifts can be several hundred or even several thousand ppm. Because of the difficulties connected with the measurement of extremely broad, severely shifted NMR signals and because of very quick nuclear spin relaxation, NMR measurements in paramagnetic MOFs are relatively rare.

### 3. Framework structure

Metal organic frameworks can comprise several NMR active nuclei, for example,  $^1\text{H}$ ,  $^{13}\text{C}$ ,  $^{14/15}\text{N}$ ,  $^{17}\text{O}$ ,  $^{19}\text{F}$ ,  $^{35}\text{Cl}$ , or  $^{79}\text{Br}$  in organic linkers and functional groups, and  $^{17}\text{O}$ ,  $^{25}\text{Mg}$ ,  $^{27}\text{Al}$ ,  $^{43}\text{Ca}$ ,  $^{45}\text{Sc}$ ,  $^{47/49}\text{Ti}$ ,  $^{51}\text{V}$ ,  $^{67}\text{Zn}$ , or  $^{91}\text{Zr}$  in metal-oxo clusters. These nuclei, especially the abundant ones and/or the ones with large magnetic moments, can be readily exploited for inspection of the framework structure. Very straightforward measurements of  $^{13}\text{C}$  and  $^1\text{H}$  NMR spectra can quickly confirm the identity of the organic linkers and the presence of functional groups attached to linker molecules [13, 14]. An example of  $^{13}\text{C}$  and  $^1\text{H}$  spectra of UiO-66, bearing different functional groups, is presented in **Figure 2**. The  $^{13}\text{C}$  spectra can clearly resolve the inequivalent aromatic and carboxyl carbon atoms. Tentative assignment of individual NMR signals to different carbon sites within the linkers, and thus the verification of the nature of the incor-

porated linker or functional groups, can often be done simply by using the 'empirical' chemical-shift-prediction programs like ChemDraw or ACD/Labs, or via the comparison of the solid-state NMR spectra with the solution NMR spectra of the corresponding linkers. Inspection of the line widths can be useful, because it provides information on the crystallinity of the materials and can alert about the presence of a local disorder in the solids.  $^1\text{H}$  and  $^{13}\text{C}$  NMR spectra also show if there are some unreacted linker molecules, water molecules and solvent molecules left in the samples.

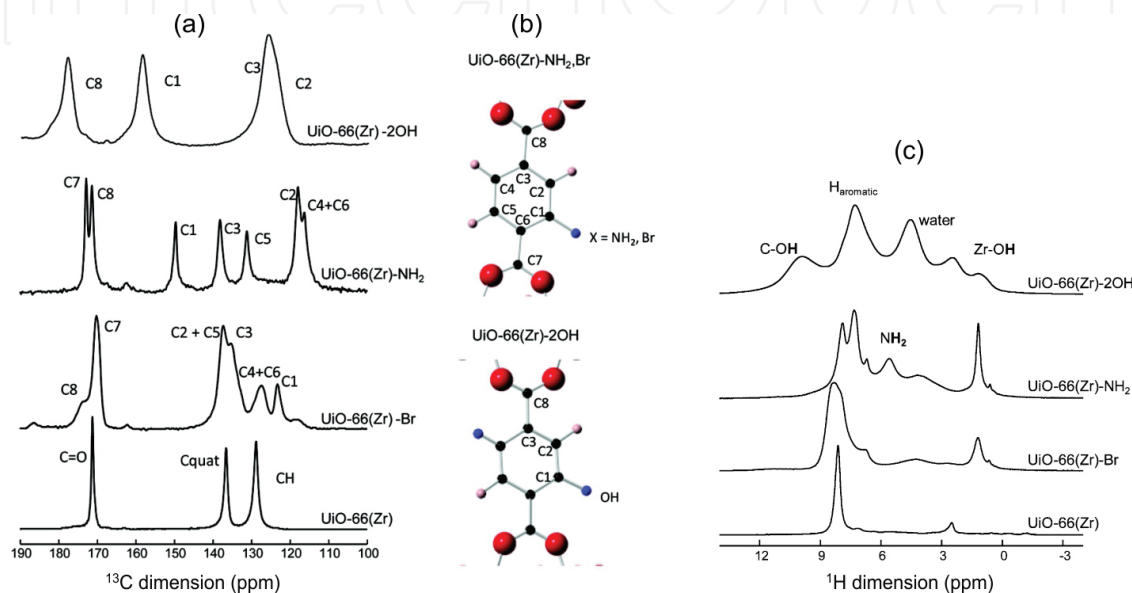


**Figure 2.** Inspection of organic linkers in differently functionalized UiO-66 materials. (a)  $^1\text{H}$ - $^{13}\text{C}$  CP-MAS and (c)  $^1\text{H}$  MAS NMR spectra. NMR signals were assigned based on DFT calculations. Labels for the individual carbon sites in the organic linkers of the NH<sub>2</sub>- and Br- (top), and 2OH- (bottom) functionalized UiO-66 are presented in (b). Broad lines in the  $^1\text{H}$ - $^{13}\text{C}$  CP-MAS spectrum of UiO-66-2OH indicate the presence of local disorder or of lower degree of crystallinity in this sample. Unlabeled  $^1\text{H}$  MAS NMR signal at about 6.5 ppm corresponds to residual ligand. Figures were published by Devautour-Vinot et al. [13]. Copyright © 2012 American Chemical Society.

Solid-state NMR can provide valuable information on the dynamics of linkers. There have been several reports on the dynamics of linkers inspected by  $^2\text{H}$  NMR spectroscopy of deuterated aromatic rings. In  $d_4$ -MOF-5, for example, it was shown that at temperature of 298 K and lower, the 1,4-phenyldicarboxylate groups were stationary, whereas at temperature of 373 K and above the aromatic rings exhibited  $\pi$ -flips about their *para* axes [15]. The onset of  $\pi$ -flips was manifested through the change of the quadrupolar line-shape of the  $^2\text{H}$  NMR signal. Similar were the findings in case of MIL-53 and MIL-47 [16]. The  $\pi$ -flips of the benzene rings were faster in the flexible MIL-53 than in the rigid MIL-47, but still not as fast as in MOF-5. It was concluded that in MIL materials with a 1D channel system, environment is considerably more constrained than in MOF-5 with a 3D system of channels. The detailed study of dynamics of benzene rings in UiO-66 showed that the temperature-dependent rotational motion affects the effective size of the windows between the pores and can thus influence the performance of the material in gas separation processes [17]. The dynamics of linkers and



functional groups can be effectively studied also by the measurements of  $^1\text{H}$  and  $^{13}\text{C}$  spin-lattice relaxation times, as was done, for example, in IRMOF-3, ZIF-4 and ZIF-8 [18, 19].

In the recent years, a substantial interest in the preparation and application of the so-called mixed-linker MOFs has arisen. Deng et al. prepared a series of MOF-5-type materials by mixing differently modified terephthalic acids in different relative amounts and combinations [20]. Altogether 18 mixed-linker MOFs with up to eight distinct functionalities in one phase were synthesized. Kong et al. employed NMR spectroscopy to obtain an insight into the distribution of different linkers [21]. They isotopically labeled various linkers used in the synthesis of MOF-5 with  $^{15}\text{N}$ , and carried out  $^{13}\text{C}$ - $^{15}\text{N}$  REDOR NMR measurements. The measurements provided information on the average distances among different linker molecules. By comparing the results of REDOR measurements with results of Monte Carlo simulations, Kong et al. were able to discriminate between cases where linkers of one type formed domains within crystals, where different linkers were alternating with one another, and where different linkers were distributed randomly throughout the crystalline framework. This valuable information helped them rationalize the observed differences in adsorption capacity and separation efficiency of mixed-linker MOFs characterized by different types of linker distributions. Another approach for studying the distribution of different linkers in mixed-linker MOFs was undertaken by Krajnc et al. [22]. They prepared Al-based metal-organic material DUT-5 with biphenyl and bipyridyl dicarboxylic molecules (bpdc and bpydc) as linkers. With two-dimensional  $^1\text{H}$ - $^{13}\text{C}$  HETCOR spectroscopy and ab-initio chemical shift calculations they successfully assigned  $^1\text{H}$  MAS NMR signals to different hydrogen atoms and showed that a peak belonging only to bpydc could be clearly resolved from a peak belonging only to bpdc. Afterward, they studied polarization transfer between these two types of hydrogen nuclei. They carried out variable-contact-time  $^1\text{H}$  spin-diffusion MAS NMR experiments and modeled spin-diffusion curves for various types of distributions of bpydc and bpdc. Comparison between the experiment and modeling allowed them to show that in their particular material the distribution of the minority bpydc linker was very homogeneous throughout the crystals and that no single-linker domains or crystallites were formed (see **Figure 3**). Both studies, the one of Kong et al. [21] and the one of Krajnc et al. [22], demonstrated that solid-state NMR spectroscopy is indeed a unique tool, capable of providing information that is not attainable by any other technique.

Aluminum is the most studied metal centre of MOFs.  $^{27}\text{Al}$  MAS NMR measurements can provide very interesting information about the framework, which is sometimes complementary to the information obtained by diffraction. Volkringer et al. employed microdiffraction and solid-state NMR to elucidate the structure of Al-MIL-100 [23]. From the X-ray diffraction (XRD) analysis, the Al-MIL-100 structure contains seven inequivalent Al crystallographic sites that belong to three distinct  $\{\text{Al}_3\text{O}(\text{OH})(\text{H}_2\text{O})_2\}_4[\text{btc}]_4$  supertetrahedra.  $^{27}\text{Al}$  MAS NMR spectrum of the as-synthesized Al-MIL-100 exhibited three overlapped signals in the chemical shift range between  $-20$  ppm and  $10$  ppm, all belonging to 6-fold coordinated aluminum sites. The signals displayed very similar isotropic chemical shifts but different quadrupolar coupling constants varying from  $1.3$  to  $5.6$  MHz. The relative areas of the three signals of 2:10:5 could be mapped onto the multiplicities of the XRD inequivalent Al sites of 2:(4:2:4):(2:1:2).

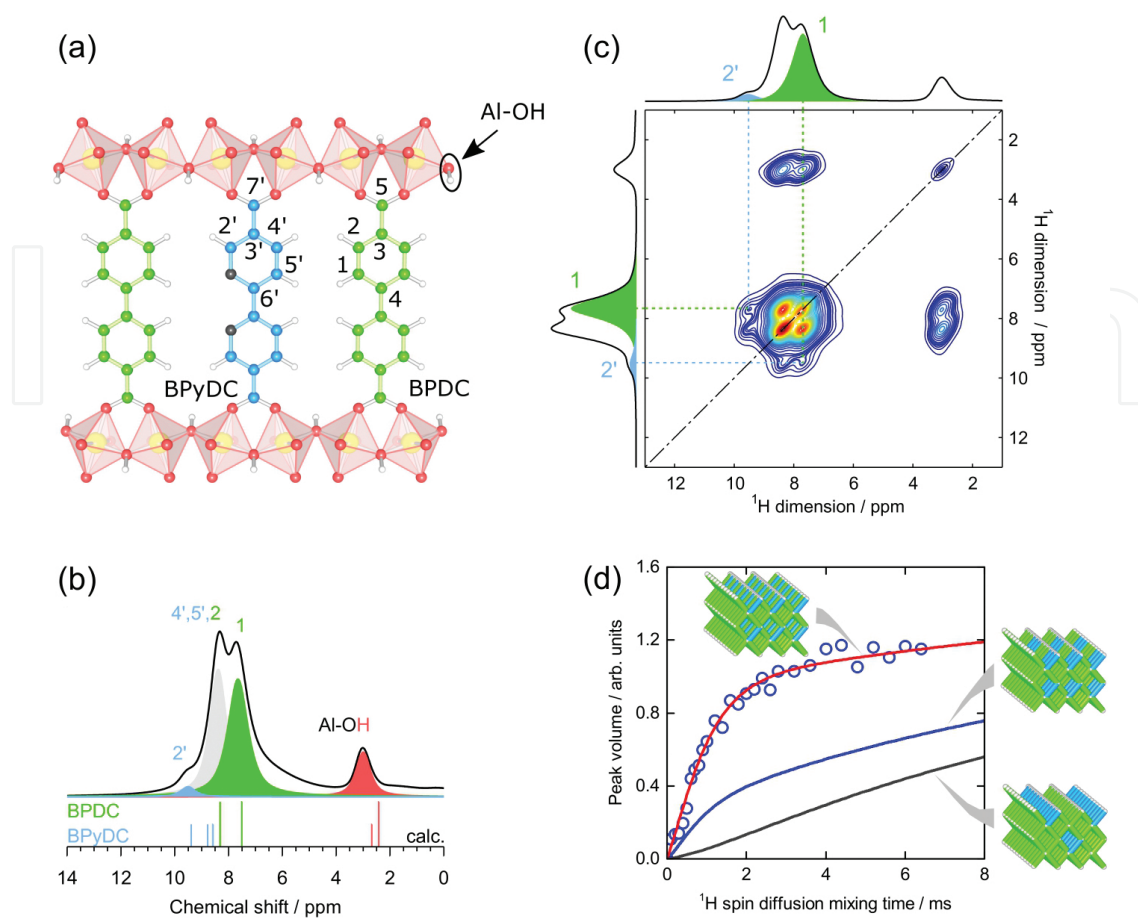


**Figure 3.** Analysis of the distribution of bpdc and bpydc linkers in the mixed-linker DUT-5 material. (a) Labeling of the framework carbon and hydrogen atoms. (b)  $^1\text{H}$  MAS NMR spectrum, which revealed that the peak belonging to bpdc (H2') can be resolved from the peak belonging to bpydc (H1). Assignment was based on DFT calculations and  $^1\text{H}$ - $^{13}\text{C}$  HETCOR NMR measurement. (c)  $^1\text{H}$  spin-diffusion homonuclear correlation NMR spectrum. Horizontal and vertical dotted lines mark the frequencies of the H2' and H1 resonances, and their crossings mark the H2'-H1 cross peaks. (d) Measured and calculated  $^1\text{H}$  spin-diffusion curves for the H2'-H1 cross peak. Results of calculations for three different models of mixed-linker DUT-5 are presented. The models are characterized by an equal bpdc/bpydc ratio but different spatial distributions of the two linkers. Only the model with a homogeneously distributed bpydc linker leads to good agreement with the experimental data. Figures were published by Krajnc et al. [22]. Copyright © 2015 Wiley-VCH.

The observed difference between NMR and XRD proportions suggested that the symmetry order was higher for NMR than for XRD. The origin of this higher symmetry was attributed to the motion of the framework protons, which led to averaging of some crystallographically distinct environments.

Very recently, first studies of  $^{67}\text{Zn}$  and  $^{25}\text{Mg}$  centers have also been described [24–29]. In these studies,  $^{67}\text{Zn}$  and  $^{25}\text{Mg}$  NMR spectroscopy mostly served as a tool for the verification of structural models of MOFs, which had been proposed by X-ray diffraction analyses. From the  $^{25}\text{Mg}$  NMR spectrum one can determine the number of crystallographically inequivalent magnesium sites (**Figure 4**), as well as chemical shift and quadrupolar coupling constant for each of these sites. Based on the proposed structural model, the same NMR observables can be calculated *ab initio*, using the gauge-included projector-augmented wave approach

(GIPAW) within the frame of the density functional theory (DFT). By comparing the measured and the calculated chemical shifts and quadrupolar coupling constants one can judge about the quality of the proposed structural models. In a recent study, Mali et al. [28] have compared the calculated and the measured  $^{13}\text{C}$  and  $^{25}\text{Mg}$  chemical shifts and  $^{25}\text{Mg}$  quadrupolar constants for a series of Mg-based MOFs. They have shown that the agreement between the calculation and the experiment was quite nice for the chemical shifts, but not for the quadrupolar coupling constants, for which the calculated values were typically substantially overestimated. The discrepancy in the calculation of electric field gradients was attributed to the dynamics of water molecules that were coordinated to the magnesium atoms. Motion of these water molecules could, namely, partially average out electric field gradients and could thus lead to apparently smaller quadrupolar couplings. Another study by Alvarez et al. showed that  $^{27}\text{Al}$  quadrupolar coupling constants in aluminum fumarate MOF A520 crucially depended on the hydration state of the material [30]. These examples thus suggest that an important role of NMR spectroscopy of metal centers could be the inspection of the coordination state of the centers and the analysis of the dynamics of the metal-oxo clusters.

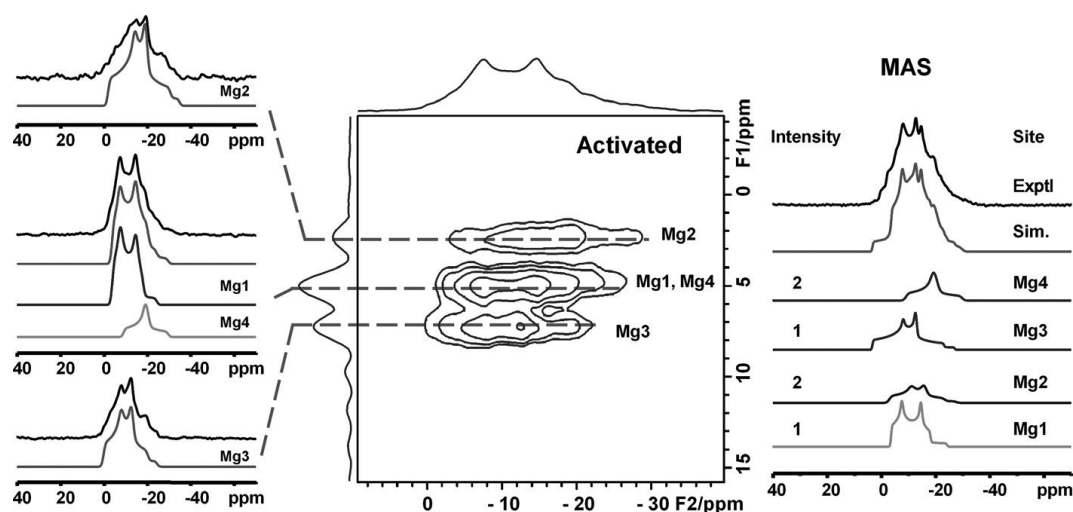


**Figure 4.** Inspection of metal centers of the activated microporous  $\alpha\text{-Mg}_3(\text{HCOO})_6$  material. Advanced two-dimensional  $^{25}\text{Mg}$  3QMAS NMR spectroscopy was employed to resolve the signals of the four inequivalent Mg sites. After the slices of the 2D spectrum were simulated (shown on the left), the obtained chemical shifts and quadrupolar coupling constants for each of the four Mg sites enabled successful simulation of the  $^{25}\text{Mg}$  MAS spectrum (shown on the right). Figures were published by Xu et al. [27]. Copyright © 2013 Wiley-VCH.

Many MOFs comprise metal centers that are paramagnetic. Such centers make NMR spectroscopy quite demanding. Even though the atomic nuclei within paramagnetic ions often do possess magnetic moments, their NMR spectra cannot be measured, because the hyperfine interactions of these nuclei with the unpaired electrons are too strong. In some cases, however, the presence of paramagnetic centers does not prevent the detection of well resolved spectra of  $^1\text{H}$  and  $^{13}\text{C}$  nuclei from linkers. One of the first examples of a detailed NMR study of paramagnetic MOFs was presented by Dawson et al. [31]. They showed  $^{13}\text{C}$  MAS NMR spectra of Cu-containing HKUST-1 and STAM-1, in which the NMR signals exhibited substantial paramagnetic shifts of up to about 800 ppm. As can be seen in **Figure 5**,  $^{13}\text{C}$  spin-lattice

relaxation times in HKUST-1 depend on the distances between the carbon atoms of the BTC linker and the copper centers, and thus enable reliable assignment of the three  $^{13}\text{C}$  signals to the three carbon sites in the linkers. The sensitivity of NMR shifts to the proximity between the NMR-active atomic nuclei and paramagnetic centers could be well exploited in the studies of mixed-metal MOFs, especially if one of the metals was paramagnetic and the other was diamagnetic. Indeed, in the case of mixed Cu-Al fluorinated MOF,  $^{19}\text{F}$  NMR detected a signal with an unusual shift of  $-456$  ppm, with large line width of 12 kHz, and with a broad manifold of spinning sidebands [32]. The signal was assigned to fluorine atoms that formed bridges between the diamagnetic aluminum and the paramagnetic copper atoms. It should be noted, however, that most of the paramagnetic centers within MOFs will give rise to much stronger paramagnetic effects than the Cu(II) ions. Especially strong effects are, for example, expected in the case of Fe(III) centers.

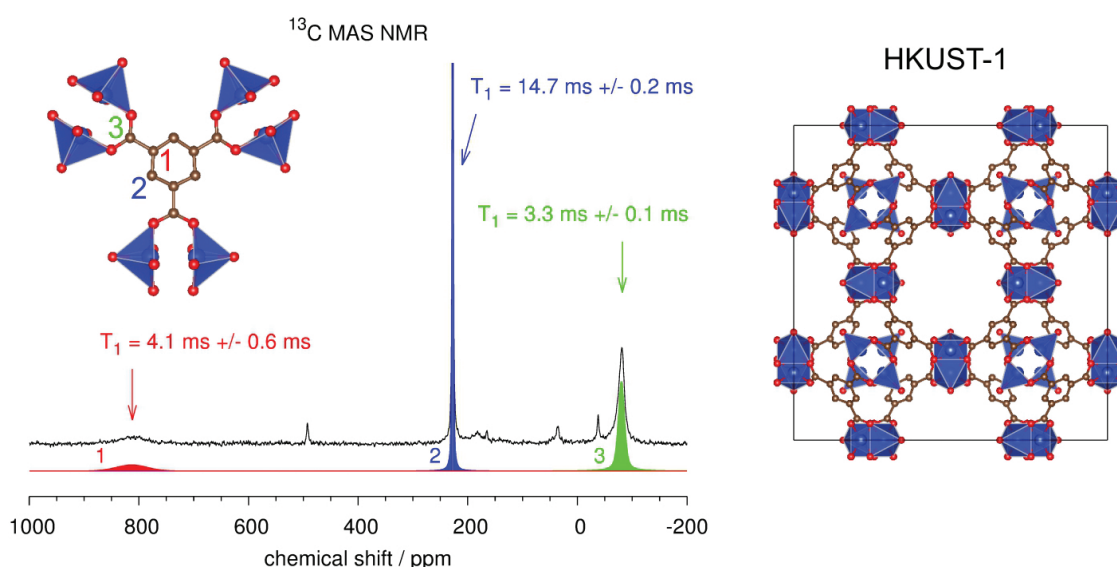


**Figure 5.** NMR analysis of the paramagnetic metal-organic framework HKUST-1. Because of the strong hyperfine interaction between the unpaired electrons and the  $^{13}\text{C}$  nuclei of the organic BTC linkers, signals in the  $^{13}\text{C}$  MAS NMR spectrum are severely shifted. Assignment of the shifted signals can be accomplished based on the corresponding  $^{13}\text{C}$  spin-lattice relaxation times  $T_1$ . The relaxation times depend on the distances between the paramagnetic centers and the  $^{13}\text{C}$  nuclei. The structure and the organic linker of HKUST-1 are schematically presented.

#### 4. Guest molecules and host-guest interactions

The role of solid-state NMR spectroscopy becomes extremely important when studying molecules within the pores of MOFs. The set of interesting species, adsorbed or incorporated into MOFs, is very large. Within this set, water is probably one of the most often studied species. Water has a strong impact on MOFs, and studying the water-framework interaction is crucial for the understanding of the MOF stability. NMR spectroscopy can be very helpful in such studies. In HKUST-1,  $^1\text{H}$  and  $^{13}\text{C}$  MAS NMR spectroscopy was employed for investigating gradual hydration of the material [33]. In spite of the fact that the copper metal centers



of HKUST-1 are paramagnetic, in the  $^1\text{H}$  MAS spectra no significant shifts of NMR signals were detected, which suggested that the electron-nucleus hyperfine couplings for  $^1\text{H}$  nuclei were rather weak. This further implied that the physico-chemical bonding of water molecules to the copper centers was weak or that adsorption and desorption of water molecules to the metal centers was very dynamic. Upon further hydration of HKUST-1, the material collapsed. The collapse of HKUST-1 due to its hydrothermal instability was evidenced by the broadening of the signals in the  $^{13}\text{C}$  MAS NMR spectrum.

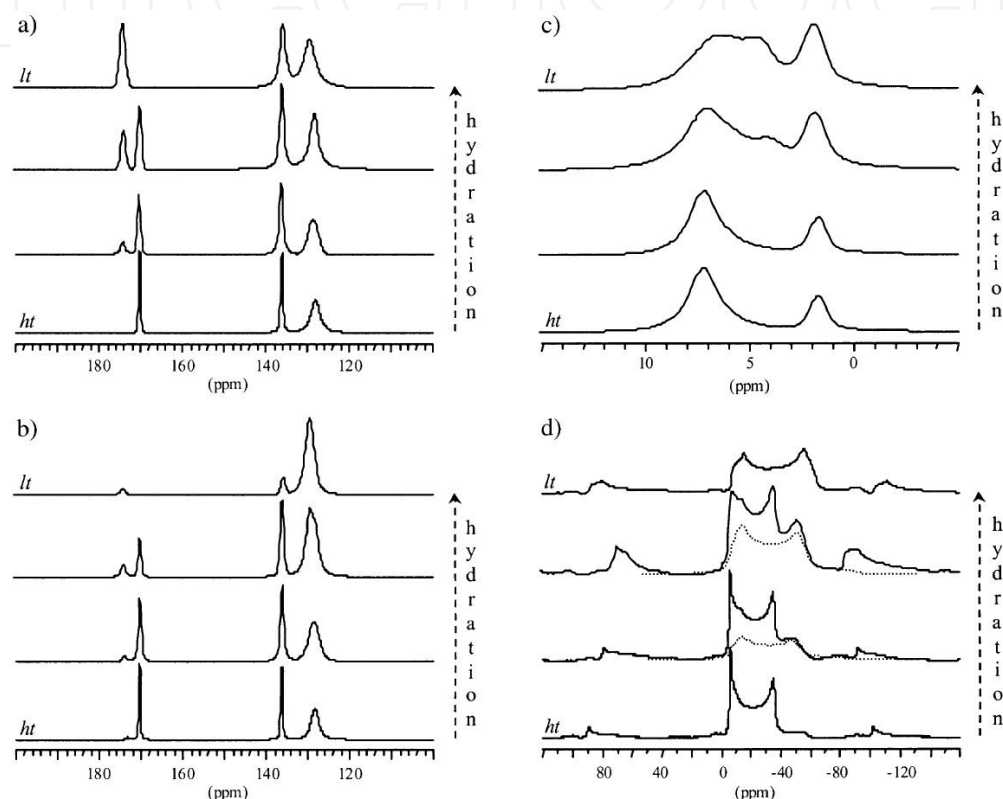


**Figure 6.** Studying hydration of Al-MIL-53. (a)  $^{13}\text{C}$  MAS, (b)  $^1\text{H}$ - $^{13}\text{C}$  CP-MAS, (c)  $^1\text{H}$  MAS, and (d)  $^{27}\text{Al}$  MAS NMR spectra of the as-prepared material (*ht* form = 'dry' material), 30% hydrated material, 50% hydrated material, and fully hydrated material (*lt* form = 'wet' material). In the  $^{27}\text{Al}$  MAS NMR spectra of the partly hydrated materials the simulated components of the wet forms are shown with dotted lines. Figures were published by Loiseau et al. [34]. Copyright © 2004 Wiley-VCH.

Several MOFs are stable in humid atmosphere or in water. Among them, Al-MIL-53 with its flexible framework is a very interesting representative. Taulelle et al. used  $^{27}\text{Al}$ ,  $^{13}\text{C}$ , and  $^1\text{H}$  MAS NMR to thoroughly inspect breathing of the material as a consequence of the reversible hydration and dehydration [34]. They showed that hydrogen bonds among the water molecules in the channels and the carboxyl groups of the linkers are responsible for the contraction of the pores upon hydration. The NMR signals of the carboxyl groups in the  $^{13}\text{C}$  MAS and  $^1\text{H}$ - $^{13}\text{C}$  CP-MAS spectra were, namely, the most affected by the presence of the water molecules. Surprisingly,  $^{27}\text{Al}$  MAS spectra showed that the bridging OH groups were practically intact during the hydration. Both,  $^{13}\text{C}$  and  $^{27}\text{Al}$  NMR spectra nicely distinguished



the contributions of the 'dry' and the 'wet' material (**Figure 6**), and allowed one to follow the gradual filling of the pores with water. Because NMR did not detect any polarization transfer between the dry and the wet material, the authors could conclude that individual crystallites in the powder were either dry or wet, but not composed of dry and wet domains. A very detailed NMR study was performed also on Al-MIL-100, which is another MOF capable of reversibly adsorbing and desorbing water [35]. The process of dehydration of Al-MIL-100 was investigated using a set of solid-state NMR techniques, including several two-dimensional homo- and heteronuclear correlation ones. The material showed a remarkable thermal stability up to 370°C. Up to 350°C, only one water molecule per aluminum-oxo trimer was found to leave the trimer, producing only one coordinatively unsaturated aluminum site among the three sites.

In the as-prepared Mg-MOF-74, the basic inorganic building units are  $\text{MgO}_6$  octahedra. In each octahedron five out of six oxygen atoms belong to the carboxylate groups of the organic linkers, and one oxygen atom belongs to a water molecule. Xu et al. showed that during the dehydration, this water molecule can be expelled from the material [26]. Whereas the dehydration did not affect the  $^{13}\text{C}$  MAS NMR spectrum, the changes in the  $^{25}\text{Mg}$  MAS NMR spectrum were quite pronounced. The  $^{25}\text{Mg}$  signal with a well-defined quadrupolar line-shape and a small quadrupolar coupling constant changed into a broad and smeared signal with a large quadrupolar coupling constant. The increase in the quadrupolar interaction was due to the change of the coordination of Mg atoms from the rather symmetrical octahedral one to the distorted square pyramidal. The smearing of the spectral line in the dehydrated material indicated that on the short-range scale the Mg environment became quite disordered. On the long-range scale, the material still exhibited an ordered porous structure. Upon rehydration of the material, the Mg local environment reversibly changed into the ordered octahedral one. The described study is particularly interesting, because in MgMOF-74 adsorption of water can compete with the adsorption of carbon dioxide. MgMOF-74 is, namely, one of the most promising materials for  $\text{CO}_2$  separation, and an interesting question of great practical importance is, how the material will perform as a sieve for carbon dioxide, if the gas mixture will contain non-negligible fraction of water.

Some hydrothermally stable MOFs can absorb very large amounts of water. Such representatives could become very interesting materials for water-adsorption based heat-storage applications. Desorption of water can be considered as an efficient energy-storage step. Upon a controlled rehydration of the dried material, large amounts of energy could be released. Again NMR spectroscopy can provide useful insight into such materials. In case of a hydrothermally stable Zn-trimesate,  $^1\text{H}$  and  $^2\text{H}$  variable-temperature MAS NMR showed that water was expelled from the material in three distinct steps (**Figure 7**) [36]. In the first step, water was desorbed from the larger pores, in the second step hydrogen-bonded water molecules from the narrow pores were expelled, and in the third step the water molecules that were coordinated to zinc atoms were desorbed. The last step occurred at about 250°C.  $^2\text{H}$  NMR spectroscopy provided additional information on the dynamics of the water molecules within the pores. Mobility of water molecules within the larger pores increased quickly with the increased temperature; their NMR signal in the  $^2\text{H}$  spectrum narrowed so that no quadrupo-

lar line-shape could be detected for this signal. On the contrary, water molecules that were coordinated to zinc atoms exhibited a well-defined quadrupolar pattern of spinning sidebands well above 100°C, meaning that motion of these water molecules was still considerably hindered at that temperature. The  $^{13}\text{C}$  spectrum recorded at 250°C was only slightly different from the spectrum of the fully hydrated material and confirmed that the framework was still well ordered at 250°C. Upon rehydration, the spectrum reversibly transformed to the initial one, showing that indeed the material was hydrothermally stable and that reversible dehydration and rehydration was possible. Recently, Cadiau et al. investigated MIL-160, which is an even more promising material for heat storage [37]. Its water uptake is as high as 320 g per 1 kg of the dry matrix. The researchers monitored gradual hydration of the dried material and detected two steps in water adsorption. Firstly, water molecules were attached to the framework hydroxyl groups on the inorganic aluminate chains, and secondly, water molecules entered into the centre of the channels. These latter water molecules did not interact appreciably with the framework.

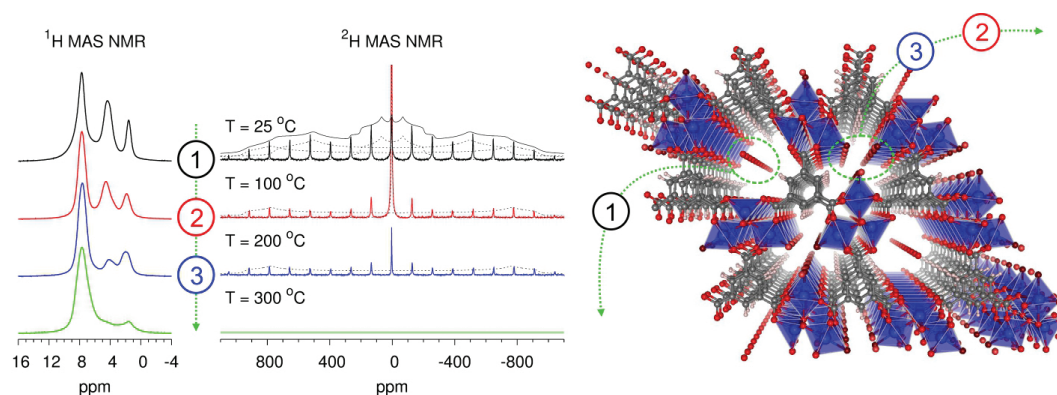


**Figure 7.** Variable-temperature  $^1\text{H}$  and  $^2\text{H}$  MAS NMR spectra of porous Zn-trimesate show that water is expelled from the material in three distinct steps. Step 1 corresponds to removal of water molecules from the larger channels, step 2 corresponds to the removal of hydrogen-bonded water molecules from the narrower channels, and step 3 corresponds to the removal of water molecules that were attached to Zn centers. In  $^1\text{H}$  MAS NMR spectra, the contribution of water molecules resonates between 4 and 5 ppm; the signal at 8 ppm belongs to H atoms of the aromatic rings of the linkers and the signal at 1–2 ppm belongs to the H atoms of the framework OH groups. In  $^2\text{H}$  MAS NMR spectra broad manifolds of spinning-sidebands correspond to rigid species, whereas high, narrow signals close to 0 ppm correspond to mobile species.

Next to water, carbon dioxide is the most interesting specie adsorbed within MOFs. Mg-MOF-74 (also termed  $\text{Mg}_2(\text{dobdc})$  or CPO-27-Mg) has been one of the most investigated systems with NMR spectroscopy. In this material, the exposed  $\text{Mg}^{2+}$  cation sites give rise to exceptional  $\text{CO}_2$  capture properties. NMR studies of Mg-MOF-74 managed to elucidate the dynamics of the adsorbed  $^{13}\text{CO}_2$  molecules [38, 39]. Analysis of static  $^{13}\text{C}$  NMR spectra quickly showed that  $^{13}\text{CO}_2$  molecules indeed bond to the  $\text{Mg}^{2+}$  sites with end-on coordination, and that the line-shape of the  $^{13}\text{C}$  signal cannot be merely a result of the spatial confinement of  $^{13}\text{CO}_2$  in the pores of Mg-MOF-74. Lin et al. carried out Monte Carlo simulations to probe equilibrium configurations of  $\text{CO}_2$  in this material [39]. Based on the calculations, they predicted that two kinds of motions of  $\text{CO}_2$  molecules are possible in the material, fluctuations of the  $\text{CO}_2$

molecule near the minimum-energy configuration and hops of the  $\text{CO}_2$  molecule between different metal sites. Considering these two types of motions, they were able to very nicely explain the measured  $^{13}\text{C}$  NMR spectra at different temperatures between 100 K and 375 K (Figure 8). At the temperature of 100 K, the pronounced  $^{13}\text{C}$  chemical shift anisotropy could be assigned exclusively to localized motions (fluctuations) of the  $^{13}\text{CO}_2$  molecules. At higher temperatures, in addition to these localized motions, also hopping of  $^{13}\text{CO}_2$  molecules between different metal sites in the plane perpendicular to the direction of the channel started to take place. With a further increase in the temperature, motion of  $^{13}\text{CO}_2$  molecules along the channel began. Lin et al. carried out equivalent  $^{13}\text{C}$  NMR measurement also on  $^{13}\text{CO}_2$  adsorbed into  $\text{Mg}_2(\text{dopbdc})$ , a material that is analogous to Mg-MOF-74, but in which separation between the neighboring magnesium sites is by 30% larger than in Mg-MOF-74 [39]. As expected, hopping motion in this material started at notably higher temperature. The study of dynamics of  $\text{CO}_2$  molecules within Mg-MOF-74 was complemented by Wang et al., who monitored variable temperature  $^{17}\text{O}$  NMR spectra of the adsorbed  $\text{C}^{17}\text{O}_2$  molecules [40].  $^{17}\text{O}$  solid-state NMR line-shapes comprise contributions from quadrupolar and chemical shift interactions, and are thus very sensitive to motions. Indeed, in the above mentioned study, the researchers were for the first time able to quantify the fourth type of motion of  $\text{CO}_2$  molecules, that is wobbling about the  $\text{CO}_2$  minimum-energy configuration.

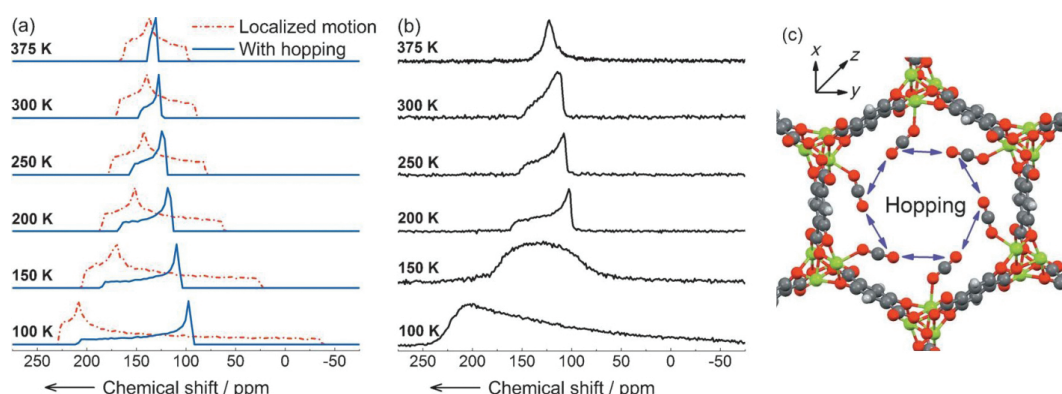


**Figure 8.** Studying dynamics of  $^{13}\text{CO}_2$  molecules adsorbed into Mg-MOF-74. (a) and (b) The comparison between the simulated and the measured static  $^{13}\text{C}$  NMR spectra, which show lines broadened by chemical shift anisotropy. The comparison indicates that at about 100 K  $\text{CO}_2$  molecules undergo localized motion around the minimum-energy positions, whereas at 200 K and above motion includes hopping of molecules between different metal sites, as indicated in (c). Figures were published by Lin et al. [39]. Copyright © 2013 Wiley-VCH.

In several MOFs,  $\text{CO}_2$  can be reversibly chemically bonded to the framework. An example of such a MOF is CD-MOF-2, for which  $^1\text{H}$ - $^{13}\text{C}$  CP-MAS NMR showed a signal at 158 ppm after the adsorption of carbon dioxide into the activated material [41]. This signal could be attributed to the carbonate that is formed upon adsorption. Other signals in the carbon spectrum, belonging to the linker molecules, were also affected by the incorporation of  $\text{CO}_2$  and thus additionally confirmed that chemical reaction between the gaseous  $\text{CO}_2$  and CD-MOF-2 took place. Let us note that the CP-MAS experiment is able to detect only rather rigid, not very mobile species, in which  $^1\text{H}$  and  $^{13}\text{C}$  nuclei are not far apart. It cannot detect the gaseous  $\text{CO}_2$ . The latter could be detected with directly excited  $^{13}\text{C}$  MAS NMR spectroscopy at about 126

ppm. The above described study concluded that the chemisorption of CO<sub>2</sub> in CD-MOF-2 relied on free hydroxyl groups, which acted as reactive hotspots for formation of carbonic acid groups. Chemisorption of CO<sub>2</sub>, more precisely formation of carbamamic acid and carbamate ions, was detected also in some modified IRMOF-74 materials [42].

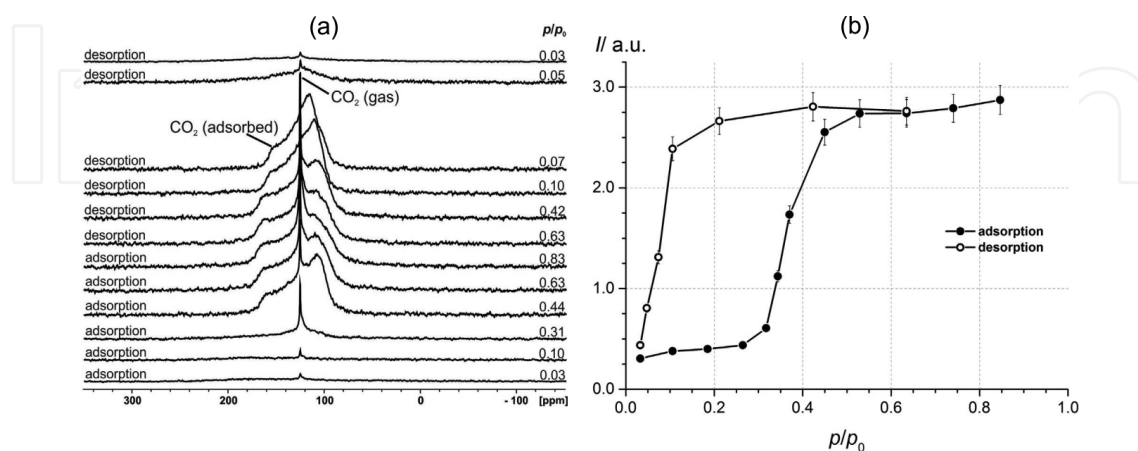


**Figure 9.** Adsorption and desorption of <sup>13</sup>CO<sub>2</sub> in [Zn<sub>2</sub>(BME-bdc)<sub>2</sub> dabco]<sub>n</sub>. <sup>13</sup>C NMR spectra (left) were recorded at *T* = 232 K and *p*<sub>0</sub> = 9.6 bar. Intensities of the adsorbed CO<sub>2</sub>, as extracted from the <sup>13</sup>C NMR spectra, are shown on the right. Figures were published by Bon et al. [43]. Copyright © 2015 Elsevier Inc.

Breathing of MIL-53 during hydration-dehydration is only one particular representation of porosity switching in this material. This more general phenomenon can be in flexible MOFs induced by changing the pressure of different gases, also of CO<sub>2</sub>. The increased pressure induces structural phase transition and increases the pores of flexible MOFs. The pressure, at which the phase transition takes place, is called the gate pressure. Bon et al. used <sup>129</sup>Xe and <sup>13</sup>C NMR spectroscopy to inspect the influence of nonpolar Xe atoms and polar CO<sub>2</sub> molecules on the porosity switching of a series of functionalized MOFs [Zn<sub>2</sub>(BME-bdc)<sub>x</sub>(DB-bdc)<sub>2-x</sub> dabco]<sub>n</sub> (*x* = 2, 1.5, 1, 0.5, 0) [43]. Whereas <sup>129</sup>Xe chemical shift is very sensitive to the confinement/ physisorption, the difference in the <sup>13</sup>C isotropic chemical shift of free CO<sub>2</sub> and of physisorbed CO<sub>2</sub> is only few ppm. However, as shown above, if motion of CO<sub>2</sub> molecules is spatially anisotropic or restricted, the corresponding <sup>13</sup>C signals can exhibit pronounced chemical shift anisotropy. In their study, Bon et al. followed <sup>13</sup>C NMR spectra while increasing the <sup>13</sup>CO<sub>2</sub> pressure (**Figure 9**). At phase transition from the narrow-pore to the large-pore form, the signal of the adsorbed <sup>13</sup>CO<sub>2</sub> narrowed and the sign of the chemical shift anisotropy changed. In different MOFs, the NMR study detected different gate pressures and different degrees of ordering of CO<sub>2</sub> molecules. Complemented by modeling, the study showed that in these MOFs without open metal sites, CO<sub>2</sub> molecules were preferentially found in the neighborhood of carboxylate carbon atoms of the linker molecules.

Water and carbon dioxide molecules are both small molecules, very important for the stability and applicability of MOFs in gas separation and storage and energy storage. Several MOFs comprise very large pores (mesopores) with the diameters of several nanometers. Into such pores also much larger molecules than H<sub>2</sub>O and CO<sub>2</sub> can be incorporated. Particularly



interesting and important examples of larger molecules are drug molecules. Indeed, very quickly after the preparation of the first large-pore MOFs, studies on the possibilities of usage of MOFs as drug-delivery matrices had begun [44, 45]. In addition to the large pore volumes of MOFs and thus to their very high drug-loading capacities, one of the most important advantages of MOFs over other potential drug-delivery matrices is the great versatility of their structures and functionalities.

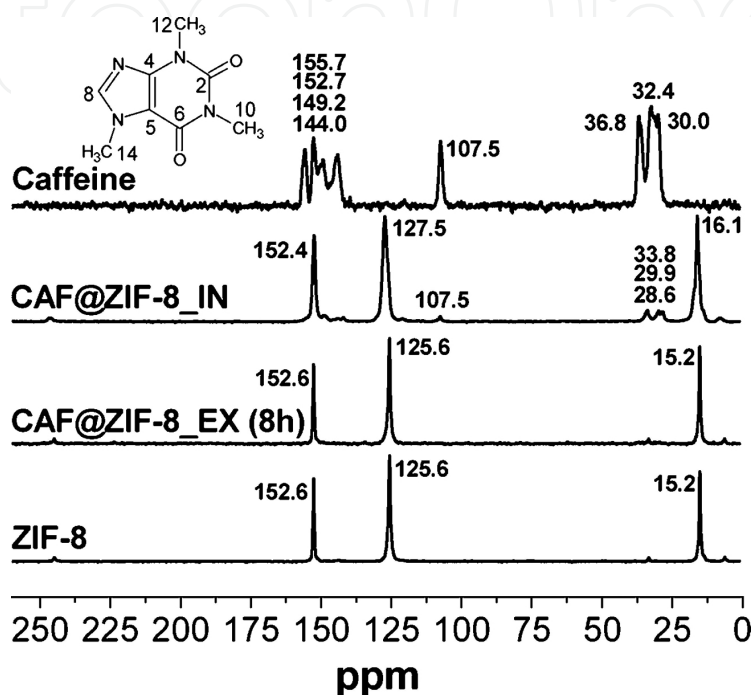


**Figure 10.**  $^1\text{H}$ - $^{13}\text{C}$  CP-MAS NMR spectra of crystalline caffeine, empty ZIF-8, and of two differently prepared drug-delivery systems. CAF@ZIF-8\_IN denotes the delivery system obtained with a one-step preparation. CAF@ZIF-8\_EX was obtained by impregnating empty ZIF-8 with an aqueous solution of caffeine for 8 h and by subsequent drying at room temperature. The detected shifts of  $^{13}\text{C}$  NMR signals of caffeine embedded into CAF@ZIF-8\_EX suggest that caffeine molecules are interacting with the ZIF-8 framework. Figure was published by Liédana et al. [46]. Copyright © 2012 American Chemical Society.

NMR spectroscopy was quite often used as a tool for obtaining the information about the nature of the incorporated drug molecules within MOFs. Very often  $^1\text{H}$  and  $^{13}\text{C}$  MAS NMR spectra of the MOFs loaded with a drug were compared to the spectra of the pure crystalline drug and of the empty MOF. The detected changes in chemical shifts of individual NMR signals could indicate, which part of the drug molecule and which part of the framework interacted one with another.  $^{13}\text{C}$  MAS NMR spectroscopy was employed for studying the incorporation of caffeine into ZIF-8 (Figure 10) [46]. Based on the shifts of the NMR signals of the caffeine's methyl group and of the 2-methylimidazole's CH group, the authors concluded that caffeine formed weak Van der Waals bonds and strong hydrogen bonds with the framework. Caffeine was incorporated also into pure UiO-66, and UiO-66 functionalized with  $\text{NH}_2$ , Br, or OH groups [47]. Detailed NMR and DFT study showed that caffeine's  $^{13}\text{C}$  chemical shift did not change after the incorporation of drug into the pores, suggesting that if there were



any interactions between caffeine molecules and the UiO frameworks, they were weak and they predominantly affected H atoms.  $^1\text{H}$  spin-lattice relaxation times for the incorporated caffeine molecules were much shorter than for the molecules within the pure crystalline caffeine. This indicated that the caffeine molecules, even though confined, were still more mobile within the pores of UiO-66 than within the caffeine crystals.  $^1\text{H}$ - $^1\text{H}$  homonuclear correlation spectra showed that only weak Van der Waals bonds between the caffeine's methyl groups and the framework's phenyl rings existed, whereas interactions with the amine and hydroxyl functional groups were not detected. The experimental findings were supported by the results of the DFT-based calculations, which proposed the energetically most favorable locations for the embedded caffeine molecules.

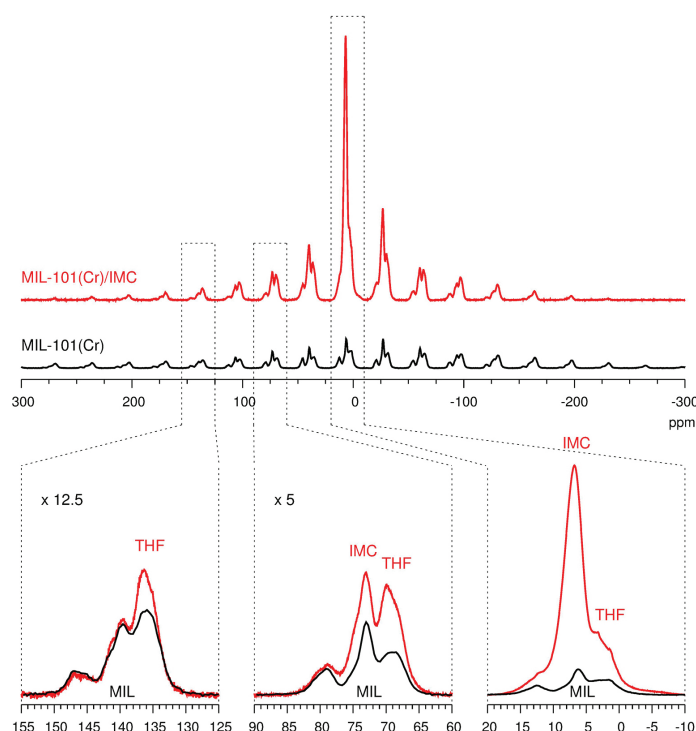


**Figure 11.**  $^1\text{H}$  MAS NMR spectra of empty MIL-101(Cr) (black) and MIL-101(Cr) loaded with indomethacin (red). Enlarged segments show the centerband next to second and forth spinning sidebands. Labels THF and IMC point to the non-negligible contributions of tetrahydrofuran (solvent) and indomethacin (drug) in the spectrum of the loaded MIL-101(Cr). Comparison of the two spectra indicates that tetrahydrofuran molecules are much more affected by the paramagnetic chromium centers than indomethacin molecules, suggesting that the former molecules are much closer to the framework metal centers than the latter molecules. Figure was published by Čendak et al. [49].

The second, quite often studied model drug is ibuprofen. Ibuprofen was incorporated into MIL-53, MIL-100, and MIL-101 [44, 48]. The most informative were  $^1\text{H}$  MAS NMR spectra, showing that in MIL-101, for example, ibuprofen was incorporated in the form of anions. Another model drug, indomethacin, was also incorporated into MIL-101. A detailed NMR study was carried out on Cr-MIL-101, Fe-MIL-101, Fe-MIL-101( $\text{NH}_2$ ), and Al-MIL-101( $\text{NH}_2$ ), into which large amounts of indomethacin were incorporated (ca. 1 g of indomethacin/1 g of an empty MIL-101 matrix) [49]. The loaded Al-MIL-101( $\text{NH}_2$ ) sample was the easiest to inspect by NMR, because its framework was diamagnetic. The measurement showed that indome-

thacin did not form strong bonds with the framework or its functional  $\text{NH}_2$  groups. Interestingly, in spite of careful drying procedure, NMR spectroscopy still detected a substantial amount of solvent tetrahydrofuran molecules within the pores of Al-MIL-101( $\text{NH}_2$ ).  $^1\text{H}$ - $^1\text{H}$  homonuclear correlation and  $^1\text{H}$ - $^{13}\text{C}$  heteronuclear correlation experiments showed that the tetrahydrofuran molecules were attached to the hydroxyl groups on the metallic trimeric units via hydrogen bonds. Very similar conclusions were obtained also for Fe- and Cr-based drug-delivery systems. In case of the Cr-MIL-101 loaded with indomethacin (and tetrahydrofuran),  $^1\text{H}$  MAS NMR spectrum clearly showed that tetrahydrofuran signals exhibited much broader pattern of spinning sidebands than indomethacin signals. This demonstrated that tetrahydrofuran was much closer to the paramagnetic chromium centers and was thus much more affected by the strong electron-nucleus dipolar coupling (**Figure 11**). It seems that strong bonding of tetrahydrofuran molecules to the metallic trimeric units and hindered transportation through the relatively narrow windows between the mesopores of MIL-101 were the reasons that drying in vacuum could not entirely remove the solvent from the pores of this potential drug-delivery matrix.

## 5. Conclusions

Selected examples of the application of solid-state NMR spectroscopy for studying MOFs showed that this spectroscopic technique can offer very valuable information about the structure and about the functioning of MOFs. Many times this information is unique and it crucially complements the information that is about MOFs obtained by other characterization tools. It is worth noting that for several of the above described studies the role of molecular modeling was particularly important. It is in fact a quite general observation that solid-state NMR spectroscopy gained a lot of power as a material's characterization tool since the introduction of modeling and accurate quantum-chemical calculations of NMR observables.

## Author details

Gregor Mali

Address all correspondence to: [gregor.mali@ki.si](mailto:gregor.mali@ki.si)

National Institute of Chemistry, Ljubljana, Slovenia

## References

- [1] Sutrisno A, Huang Y. Solid-state NMR: A powerful tool for characterization of metal-organic frameworks. *Solid State Nuclear Magnetic Resonance*. 2013 Feb;49–50:1–11.

- [2] Hoffmann HC, Debowski M, Müller P, Paasch S, Senkovska I, Kaskel S, et al. Solid-state NMR spectroscopy of metal-organic framework compounds (MOFs). *Materials*. 2012 Nov 28;5(12):2537–72.
- [3] Andrew ER, Bradbury A, Eades RG. Nuclear magnetic resonance spectra from a crystal rotated at high speed. *Nature*. 1958 Dec 13;182(4650):1659–1659.
- [4] Pines A, Gibby MG, Waugh JS. Proton-enhanced NMR of dilute spins in solids. *J. Chem. Phys.* 1973 Jul 15;59(2):569–590.
- [5] Carr HY, Purcell EM. Effects of diffusion on free precession in nuclear magnetic resonance experiments. *Phys Rev.* 1954 May 1;94(3):630–638.
- [6] O'Dell LA, Schurko RW. QCPMG using adiabatic pulses for faster acquisition of ultra-wideline NMR spectra. *Chem Phys Lett.* 2008 Oct 13;464(1–3):97–102.
- [7] Bennett AE, Griffin RG, Ok JH, Vega S. Chemical shift correlation spectroscopy in rotating solids: radio frequency-driven dipolar recoupling and longitudinal exchange. *J Chem Phys.* 1992 Jun 1;96(11):8624–8627.
- [8] Feike M, Demco DE, Graf R, Gottwald J, Hafner S, Spiess HW. Broadband multiple-quantum NMR spectroscopy. *J Magn Resonance, Ser A.* 1996 Oct;122(2):214–221.
- [9] Hohwy M, Jakobsen HJ, Edén M, Levitt MH, Nielsen NC. Broadband dipolar recoupling in the nuclear magnetic resonance of rotating solids: a compensated C7 pulse sequence. *J Chem Phys.* 1998 Feb 15;108(7):2686–2694.
- [10] van Rossum B-J, Förster H, de Groot HJM. High-field and high-speed CP-MAS13C NMR heteronuclear dipolar-correlation spectroscopy of solids with frequency-switched Lee–Goldburg homonuclear decoupling. *J Mag Resonance.* 1997 Feb;124(2):516–519.
- [11] Mao K, Pruski M. Directly and indirectly detected through-bond heteronuclear correlation solid-state NMR spectroscopy under fast MAS. *J Magn Resonance.* 2009 Dec;201(2):165–174.
- [12] Gullion T, Schaefer J. Rotational-echo double-resonance NMR. *J Magn Resonance* (1969). 1989 Jan 1;81(1):196–200.
- [13] Devautour-Vinot S, Maurin G, Serre C, Horcajada P, Paula da Cunha D, Guillerm V, et al. Structure and dynamics of the functionalized MOF type UiO-66(Zr): NMR and dielectric relaxation spectroscopies coupled with DFT calculations. *Chem Mater.* 2012 Jun 12;24(11):2168–2177.
- [14] Wittmann T, Siegel R, Reimer N, Milius W, Stock N, Senker J. Enhancing the water stability of Al-MIL-101-NH<sub>2</sub> via postsynthetic modification. *Chem Eur J.* 2015 Jan 2;21(1):314–323.

- [15] Gonzalez J, Nandini Devi R, Tunstall DP, Cox PA, Wright PA. Deuterium NMR studies of framework and guest mobility in the metal-organic framework compound MOF-5,  $\text{Zn}_4\text{O}(\text{O}_2\text{CC}_6\text{H}_4\text{CO}_2)_3$ . *Microporous Mesoporous Mater.* 2005 Sep 15;84(1–3):97–104.
- [16] Kolokolov DI, Jobic H, Stepanov AG, Guillerm V, Devic T, Serre C, et al. Dynamics of benzene rings in MIL-53(Cr) and MIL-47(V) frameworks studied by  $^2\text{H}$  NMR spectroscopy. *Angew Chem Int Ed.* 2010 Jun 28;49(28):4791–4794.
- [17] Kolokolov DI, Stepanov AG, Guillerm V, Serre C, Frick B, Jobic H. Probing the dynamics of the porous Zr terephthalate UiO-66 framework using  $^2\text{H}$  NMR and neutron scattering. *J Phys Chem C.* 2012 Jun 7;116(22):12131–12136.
- [18] Morris W, Taylor RE, Dybowski C, Yaghi OM, Garcia-Garibay MA. Framework mobility in the metal-organic framework crystal IRMOF-3: evidence for aromatic ring and amine rotation. *J Mol Struct.* 2011 Oct 12;1004(1–3):94–101.
- [19] Morris W, Stevens CJ, Taylor RE, Dybowski C, Yaghi OM, Garcia-Garibay MA. NMR and X-ray Study revealing the rigidity of zeolitic imidazolate frameworks. *J Phys Chem C.* 2012 Jun 21;116(24):13307–13312.
- [20] Deng H, Doonan CJ, Furukawa H, Ferreira RB, Towne J, Knobler CB, et al. Multiple functional groups of varying ratios in metal-organic frameworks. *Science.* 2010 Feb 12;327(5967):846–850.
- [21] Kong X, Deng H, Yan F, Kim J, Swisher JA, Smit B, et al. Mapping of functional groups in metal-organic frameworks. *Science.* 2013;341(6148):882–885.
- [22] Krajnc A, Kos T, Zabukovec Logar N, Mali G. A simple NMR-based method for studying the spatial distribution of linkers within mixed-linker metal-organic frameworks. *Angew Chem Int Ed.* 2015 Sep 1;54(36):10535–10538.
- [23] Volkringer C, Popov D, Loiseau T, Férey G, Burghammer M, Riekel C, et al. Synthesis, single-crystal X-ray microdiffraction, and NMR characterizations of the giant pore metal-organic framework aluminum trimesate MIL-100. *Chem Mater.* 2009 Dec 22;21(24):5695–5697.
- [24] Sutrisno A, Terskikh VV, Shi Q, Song Z, Dong J, Ding SY, et al. Characterization of Zn-containing metal-organic frameworks by solid-state  $^{67}\text{Zn}$  NMR spectroscopy and computational modeling. *Chem Eur J.* 2012 Sep 24;18(39):12251–12259.
- [25] He P, Lucier BEG, Terskikh VV, Shi Q, Dong J, Chu Y, et al. Spies within metal-organic frameworks: investigating metal centers using solid-state NMR. *J Phys Chem C.* 2014 Oct 16;118(41):23728–23744.
- [26] Xu J, Terskikh VV, Huang Y.  $^{25}\text{Mg}$  solid-state NMR: a sensitive probe of adsorbing guest molecules on a metal center in metal-organic framework CPO-27-Mg. *J Phys Chem Lett.* 2013 Jan 3;4(1):7–11.

- [27] Xu J, Terskikh VV, Huang Y. Resolving multiple non-equivalent metal sites in magnesium-containing metal-organic frameworks by natural abundance  $^{25}\text{Mg}$  solid-state NMR spectroscopy. *Chem Eur J*. 2013 Apr 2;19(14):4432–4436.
- [28] Mali G, Trebosc J, Martineau C, Mazaj M. Structural study of Mg-based metal-organic frameworks by X-ray diffraction,  $^1\text{H}$ ,  $^{13}\text{C}$ , and  $^{25}\text{Mg}$  solid-state NMR spectroscopy, and first-principles calculations. *J Phys Chem C*. 2015 Apr 9;119(14):7831–7841.
- [29] Xu J, Lucier BEG, Sinelnikov R, Terskikh VV, Staroverov VN, Huang Y. Monitoring and understanding the paraelectric–ferroelectric phase transition in the metal-organic framework  $[\text{NH}_4][\text{M}(\text{HCOO})_3]$  by solid-state NMR spectroscopy. *Chem Eur J*. 2015 Oct 5;21(41):14348–14361.
- [30] Alvarez E, Guillou N, Martineau C, Bueken B, Van de Voorde B, Le Guillouzer C, et al. The structure of the aluminum fumarate metal-organic framework A520. *Angew Chem Int Ed*. 2015 Mar 16;54(12):3664–3668.
- [31] Dawson DM, Jamieson LE, Mohideen MIH, McKinlay AC, Smellie IA, Cadou R, et al. High-resolution solid-state  $^{13}\text{C}$  NMR spectroscopy of the paramagnetic metal-organic frameworks, STAM-1 and HKUST-1. *Phys Chem Chem Phys*. 2012 Dec 13;15(3):919–929.
- [32] Cadiau A, Auguste S, Taulelle F, Martineau C, Adil K. Hydrothermal synthesis, ab-initio structure determination and NMR study of the first mixed Cu–Al fluorinated MOF. *CrystEngComm*. 2013 Apr 2;15(17):3430–3435.
- [33] Gul-E-Noor F, Jee B, Pöppl A, Hartmann M, Himsl D, Bertmer M. Effects of varying water adsorption on a  $\text{Cu}_3(\text{BTC})_2$  metal-organic framework (MOF) as studied by  $^1\text{H}$  and  $^{13}\text{C}$  solid-state NMR spectroscopy. *Phys Chem Chem Phys*. 2011 Apr 14;13(17):7783–7788.
- [34] Loiseau T, Serre C, Huguenard C, Fink G, Taulelle F, Henry M, et al. A rationale for the large breathing of the porous aluminum terephthalate (MIL-53) upon hydration. *Chem Eur J*. 2004 Mar 19;10(6):1373–1382.
- [35] Haouas M, Volkringer C, Loiseau T, Férey G, Taulelle F. Monitoring the activation process of the giant pore MIL-100(Al) by solid state NMR. *J Phys Chem C*. 2011 Sep 15;115(36):17934–1744.
- [36] Birsa Čelič T, Mazaj M, Guillou N, Elkaïm E, El Roz M, Thibault-Starzyk F, et al. Study of hydrothermal stability and water sorption characteristics of 3-dimensional Zn-based trimesate. *J Phys Chem C*. 2013 Jul 18;117(28):14608–14617.
- [37] Cadiau A, Lee JS, Damasceno Borges D, Fabry P, Devic T, Wharmby MT, et al. Design of hydrophilic metal organic framework water adsorbents for heat reallocation. *Adv Mater*. 2015 Aug 1;27(32):4775–4780.



- [38] Kong X, Scott E, Ding W, Mason JA, Long JR, Reimer JA. CO<sub>2</sub> dynamics in a metal-organic framework with open metal sites. *J Am Chem Soc.* 2012 Sep 5;134(35):14341–14344.
- [39] Lin L-C, Kim J, Kong X, Scott E, McDonald TM, Long JR, et al. Understanding CO<sub>2</sub> dynamics in metal-organic frameworks with open metal sites. *Angew Chem Int Ed.* 2013 Apr 15;52(16):4410–4413.
- [40] Wang WD, Lucier BEG, Terskikh VV, Wang W, Huang Y. Wobbling and hopping: studying dynamics of CO<sub>2</sub> adsorbed in metal-organic frameworks via <sup>17</sup>O solid-state NMR. *J Phys Chem Lett.* 2014 Oct 2;5(19):3360–3365.
- [41] Gassensmith JJ, Furukawa H, Smaldone RA, Forgan RS, Botros YY, Yaghi OM, et al. Strong and reversible binding of carbon dioxide in a green metal-organic framework. *J Am Chem Soc.* 2011 Oct 5;133(39):15312–15315.
- [42] Sung Cho H, Deng H, Miyasaka K, Dong Z, Cho M, Neimark AV, et al. Extra adsorption and adsorbate superlattice formation in metal-organic frameworks. *Nature.* 2015 Nov 26;527(7579):503–507.
- [43] Bon V, Pallmann J, Eisbein E, Hoffmann HC, Senkovska I, Schwedler I, et al. Characteristics of flexibility in metal-organic framework solid solutions of composition [Zn<sub>2</sub>(BME-bdc)<sub>x</sub>(DB-bdc)<sub>2-x</sub>dabco]<sub>n</sub>: In situ powder X-ray diffraction, in situ NMR spectroscopy, and molecular dynamics simulations. *Microporous Mesoporous Mater.* 2015 Nov 1;216:64–74.
- [44] Horcajada P, Serre C, Maurin G, Ramsahye NA, Balas F, Vallet-Regí M, et al. Flexible porous metal-organic frameworks for a controlled drug delivery. *J Am Chem Soc.* 2008 May 1;130(21):6774–6780.
- [45] Horcajada P, Chalati T, Serre C, Gillet B, Sebrie C, Baati T, et al. Porous metal-organic-framework nanoscale carriers as a potential platform for drug delivery and imaging. *Nat Mater.* 2010 Feb;9(2):172–178.
- [46] Liédana N, Galve A, Rubio C, Téllez C, Coronas J. CAF@ZIF-8: one-step encapsulation of cCaffeine in MOF. *ACS Appl Mater Interfaces.* 2012 Sep 26;4(9):5016–5021.
- [47] Devautour-Vinot S, Martineau C, Diaby S, Ben-Yahia M, Miller S, Serre C, et al. Caffeine confinement into a series of functionalized porous zirconium MOFs: a joint experimental/modeling exploration. *J Phys Chem C.* 2013 Jun 6;117(22):11694–11704.
- [48] Horcajada P, Serre C, Vallet-Regí M, Sebban M, Taulelle F, Férey G. Metal-organic frameworks as efficient materials for drug delivery. *Angew Chem Int Ed.* 2006 Sep 11;45(36):5974–5978.
- [49] Čendak T, Žunkovič E, Godec TU, Mazaj M, Logar NZ, Mali G. Indomethacin embedded into MIL-101 frameworks: a solid-state NMR study. *J Phys Chem C.* 2014 Mar 27;118(12):6140–6150.

